



# Gas flow rate distributions in parallel minichannels for polymer electrolyte membrane fuel cells: Experiments and theoretical analysis

Lifeng Zhang<sup>a</sup>, Hsiaotao T. Bi<sup>a,\*</sup>, David P. Wilkinson<sup>a</sup>, Jürgen Stumper<sup>b</sup>, Haijiang Wang<sup>c</sup>

<sup>a</sup> Department of Chemical and Biological Engineering, The University of British Columbia, 2360 East Mall, Vancouver, V6T 1Z3 BC, Canada

<sup>b</sup> Automotive Fuel Cell Corporation, 9000 Glenlyon Parkway, Burnaby, V5J 5J8 BC, Canada

<sup>c</sup> NRC Institute of Fuel Cell Innovation, Vancouver, Canada

## ARTICLE INFO

### Article history:

Received 16 October 2009

Received in revised form

22 November 2009

Accepted 25 November 2009

Available online 2 December 2009

### Keywords:

Gas flow rate distribution

Gas–liquid two-phase flow

Parallel channel

Flow instability

Flow hysteresis

Fuel cells

## ABSTRACT

In the present work, instantaneous gas flow rates in each of two parallel channels of gas–liquid two-phase flow systems were investigated through measurements of the pressure drop across the entrance region. Liquid flow rates in two branches were pre-determined through liquid injection independently into each channel. Experiments were conducted in two different manners, i.e., the gas flow rate was varied in both ascending and descending paths. Flow hysteresis was observed in both gas flow rate distributions and the overall pressure drop of two-phase flow systems. Effects of liquid flow rates on gas flow distributions were examined experimentally. The presence of flow hysteresis was found to be associated with different flow patterns at different combinations of gas and liquid flow rates and flow instability conditions. A new and simple method was developed to predict gas flow distributions based on flow regime-specific pressure drop models for different experimental approaches and flow patterns. In particular, two different two-phase pressure drop models were used for slug flow and annular flow, separately. Good agreement was achieved between the theoretical predictions and our experimental data. The developed new method can be potentially applied to predict gas flow distributions in parallel channels for fuel cells.

© 2009 Elsevier B.V. All rights reserved.

## 1. Introduction

Gas liquid two-phase flow in parallel channels has been found in many engineering applications such as heat exchangers, nuclear reactors, etc. Recently, it has received increasing attention due to its applications in PEM fuel cells. The flow fields of PEM fuel cells typically consist of parallel channels with diameters of sub-millimeters. Those parallel channels usually share the same manifold inlet and outlet. Water is generated as the by-product of the electrochemical reaction taking place at the active catalyst surface and diffuses through the gas diffusion layer to gas flow channels, removed by the gas stream. Gas streams are usually humidified at the inlet in order to achieve an efficient operation and therefore the presence of liquid water is unavoidable due to water saturation and condensation in operating fuel cells. In general, liquid water emerges from the gas diffusion layer as droplets and accumulates along the gas flow channel and forms liquid slugs before purged out by gas. In order to maintain efficient operations, the liquid water requires instantaneous removal because the liquid slugs could flood gas flow channels and GDLs and block the passage of gas reactants to catalyst surfaces and too much water also degrades catalyst.

In addition, the presence of liquid slugs also could lead to flow mal-distribution. One channel might be clogged with liquid slugs while the others might be dried out due to excessive amount of gas flow. As a direct consequence, flow mal-distribution leads to current re-distribution, erratic current fluctuations, and pressure drop fluctuations. Gas flow mal-distribution in active fuel cells has been reported through transparent *in situ* experiments [1,2]. Numerical simulations have also been conducted to predict two-phase flow distributions in parallel channels [3]. However, in the literature, a sound theoretical foundation is still lacking to interpret flow mal-distribution of two-phase flow in parallel channels. In flow field design for PEM fuel cells, the flow distribution is mainly based on the single-phase flow, where flow resistance or pressure drop is directly related to flow rates. However, the flow distribution of two-phase systems is much more complicated. In our recent work, it was observed that various flow distribution combinations of two-phase flow rates could give the same pressure drop based on measured water distribution in two parallel channels [4]. Given the challenging nature of measurement of gas flow rate distribution in parallel channels, only recently Lu et al. [5] and Kandlikar et al. [6] measured gas flow rates based on the pressure drop over the entrance region where there is no water present. However, no theoretical analysis has been conducted to predict gas flow rates in individual channels. In addition, effect of experimental methods on gas flow distributions has not been explored. According to previous studies

\* Corresponding author. Tel.: +1 604 822 4408; fax: +1 604 822 6003.  
E-mail address: [xbi@chbe.ubc.ca](mailto:xbi@chbe.ubc.ca) (H.T. Bi).

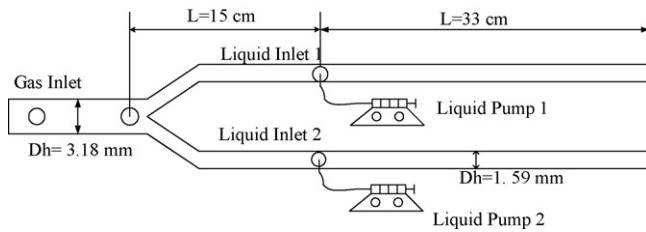


Fig. 1. Schematics of the experimental set-up.

[7,8], different flow patterns of two-phase flow in parallel channels were observed when varying gas flow rates in ascending and descending orders. This implies that in actual fuel cell operations, the manners of variations in gas flow rates or gas stoichiometries could potentially play an important role in power performance. This is not well addressed in fuel cell design and operation, especially, from two-phase flow perspectives. Therefore, in the present work, an attempt has been made to advance our understanding of two-phase flow and flow distributions in parallel channels under flow conditions related to fuel cell operations by directly measuring gas flow distributions in two parallel channels. In addition, a novel approach was attempted to predict flow distributions based on flow pattern-dependent pressure drop models.

## 2. Experiments

Experiments were conducted in a Y-branched parallel channel system with a square cross-section with a diameter of 1.59 mm by 1.59 mm. Pressure drop was measured at the entrance region in each branched channel with a length of 15 cm as shown in Fig. 1. Liquid water was introduced 15 cm after the entrance region. Two syringe pumps were employed to supply liquid water to two channels at either the same or different liquid flow rates. The two-phase flow region has a length of 33 cm in both channels. In the experiments, the gas flow rate was varied following two different orders, ascending and descending.

To measure gas flow rate into each bifurcated channel in the Y-branch system, pressure drop at the entrance section of each branch was first measured by blocking the other branch in the absence of water injection, with the results shown in Fig. 2. Although the pressure drop measured at each branch includes contributions from bifurcation from the head manifold to individual channels, for purposes of simplicity, the pressure vs. flow rate data in Fig. 2 were fitted to polynomial equations.

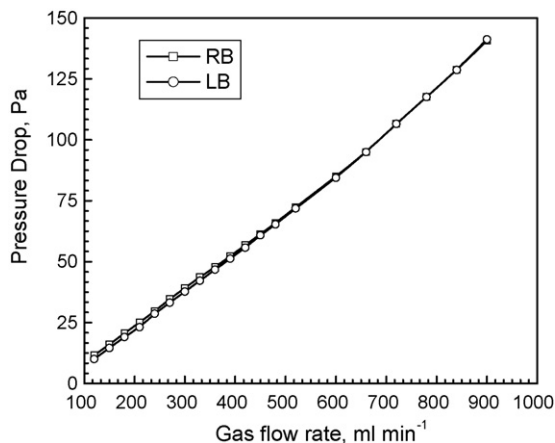


Fig. 2. Pressure drop of a single-phase gas flow at the entrance regions of two branches.

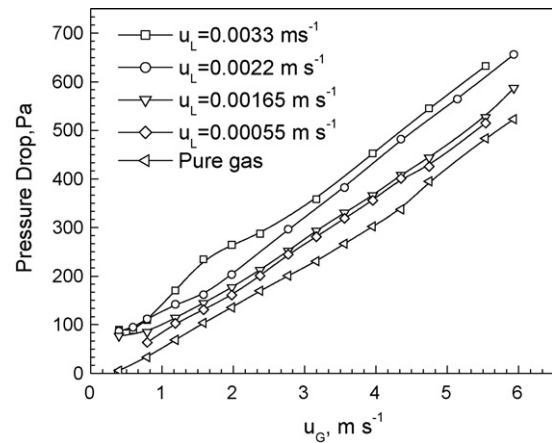


Fig. 3. Pressure drop of two-phase flow in a single branch.

For the right branch:

$$\Delta P_{RB} = 3E - 5Q^2 + 0.128Q \quad (1)$$

and for the left branch:

$$\Delta P_{LB} = 3E - 5Q^2 + 0.131Q \quad (2)$$

It can be seen that there is little difference between two channels and the slight difference will play a marginal role in causing mal-distribution of gas into the two parallel channels. Eqs. (1) and (2) were thus used in this study to estimate actual gas flow rates in individual channels at given flow conditions with liquid injection based on in situ pressure drop data when liquid was introduced.

In addition, the pressure drop of gas–liquid two-phase flows in a single branch at different flow rates was also measured with the other channel blocked to establish a baseline for two-phase flow in a single channel. As shown in Fig. 3, the pressure drop of a two-phase flow is always higher than the single-phase gas flow system.

## 3. Results and discussion

### 3.1. Effects of liquid injection into one channel on gas flow distributions

In an extreme case for two-phase parallel flow channels, single-phase liquid flow appears in one channel and single-phase gas flow or two-phase mist flow in the other channel [8], resembling a scenario that all liquid water accumulates in one channel of a fuel cell flow field, leaving other channels dehydrated. To investigate such an extreme case, liquid water was only injected to one channel and gas flow rates were varied in both ascending and descending orders. Gas flow rate into each channel was estimated using Eqs. (1) and (2) with typical flow distributions and corresponding pressure drops over the test section of two-phase flow ( $L = 33$  cm) for both gas ascending and descending processes shown in Fig. 4. In order to balance the pressure drop in two parallel channels, the majority of gas flows through the dry-out channel and only a small amount of gas enters the channel filled with water, resulting in a bubbly flow or slug flow pattern in the channel with water injection and a single-phase gas flow in the other channel. When the total gas flow rate reaches a value of about  $1030 \text{ ml min}^{-1}$ , the gas flow rate in the dry-out channel suddenly drops to around  $600 \text{ ml min}^{-1}$  with the rest of gas flowing into the flooded channel, resulting in a transition of flow pattern from bubbly/slug flow to annular/stratified flow there. When the gas flow rate was varied in the descending path as indicated in Fig. 4(a),

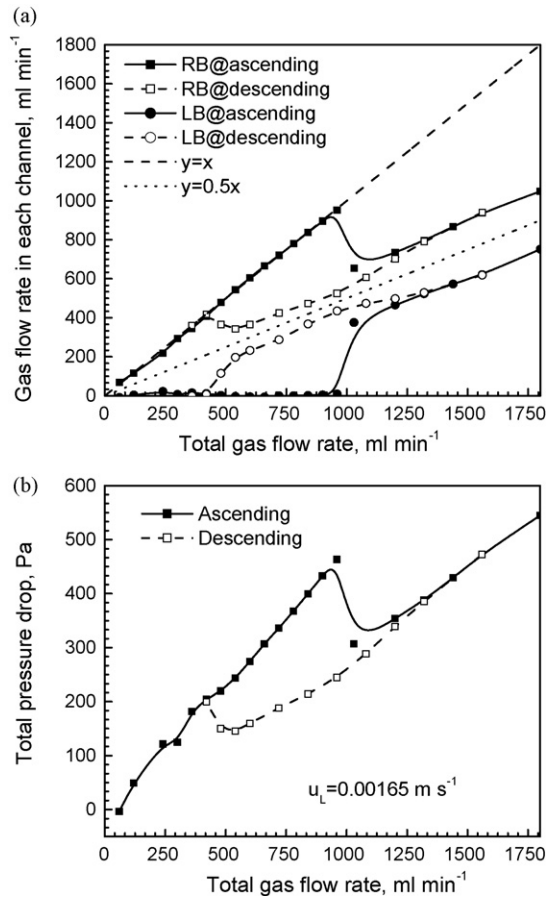


**Fig. 4.** (a) Gas flow rate in each channel and (b) total pressure drop as a function of total gas flow rate with  $u_L = 0.00165 \text{ m s}^{-1}$  in the left branch (LB); solid line represents ascending path and dotted line represents descending path.

the trajectory of gas flow distributions is distinctly different from that following a gas ascending path, rendering a flow hysteresis phenomenon. Such a unique flow hysteresis phenomenon of two-phase flow in parallel channels seems to be consistent with those reported in the literature based on measured pressure drops [7,8], as shown in Fig. 4(b). However, current experimental configuration of controlled liquid injection into each channel enables us to show that the presence of flow hysteresis in gas flow distributions is directly linked to the hysteresis in pressure drop vs. total gas flow rate curves, and is caused by the difference in the flow patterns encountered during the gas ascending and descending processes. In the gas ascending process, bubbly and slug flows are obtained at low gas flow rates and transition to annular or stratified flows takes place at relatively high gas flow rate, triggering a sudden shift in the gas flow distribution in Fig. 4(a), which is likely associated with the instability of slug flow. At the same time, a sudden change in total pressure drop occurs at the same gas flow rate when flow distributions are suddenly changed, as shown in Fig. 4(b).

As the liquid flow into the left branch was increased to  $0.0033 \text{ m s}^{-1}$ , Fig. 5 shows that the sudden flow distribution in the gas ascending process occurred at a higher gas flow rate ( $\sim 1320 \text{ ml min}^{-1}$ ) than in Fig. 4(a) because the transition from slug flow to annular/stratified flow for a higher liquid flow rate appears at a higher gas velocity.

If the liquid flow rate is lowered, as expected, the flow hysteresis occurs within a narrower gas flow range as shown in Fig. 6 for a liquid velocity of  $0.00055 \text{ m s}^{-1}$  in the left channel.

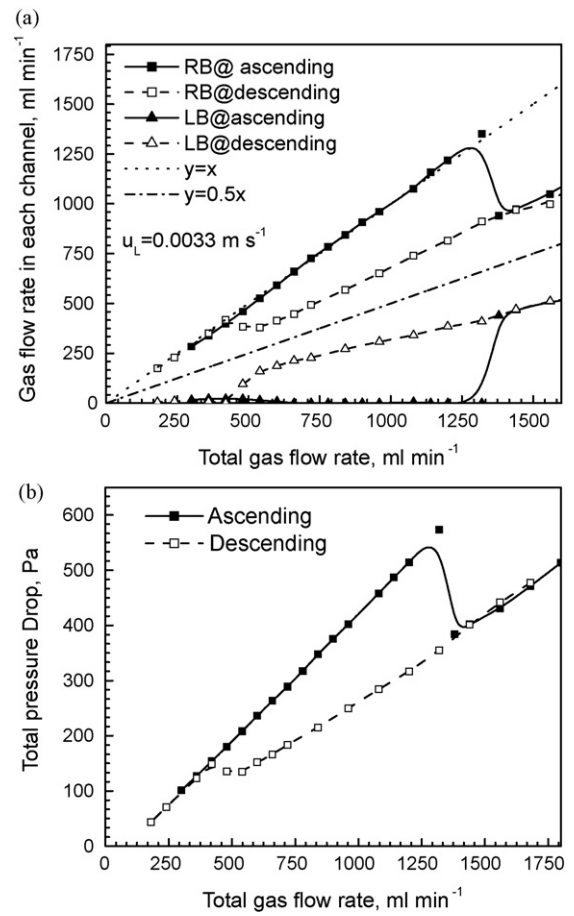


**Fig. 5.** (a) Gas flow rate in each channel and (b) total pressure drop with  $u_L = 0.0033 \text{ m s}^{-1}$  in the left channel as a function of total gas flow rate; solid line represents ascending approach and dashed line represents descending approach.

### 3.2. Effects of non-uniform liquid injection on gas flow distributions

Different from the previous section, water was now injected into both channels at either the same or different flow rates. Representative flow distributions and their corresponding total pressure drop are given in Fig. 7 with equal liquid injection rate into both channels.

It can be seen in Fig. 7(a) that even gas flow distribution occurs at a higher gas flow rate in the gas ascending process compared to the descending path. At the high gas flow rates, gas flow rate in each parallel channel is close to the line of  $y=0.5x$ , indicating an approximately even gas flow distribution in the two parallel channels. The pressure drop hysteresis appears in the region where there is a sudden change in gas flow from uniform to non-uniform distribution, similar to what observed when there is a non-uniform liquid injection into the two channels.

At a lower liquid flow rate of equal distribution, Fig. 8(a) shows that the sudden changes of gas flow distributions and the corresponding pressure drop occur at a total gas flow rate of around  $480 \text{ ml min}^{-1}$  in Fig. 8(b), lower than at higher liquid flow rate, due to earlier flow pattern transition from slug flow to annular flow. The presence of sudden shift in both gas flow distribution and the pressure drop implies that a single pressure drop model might not work for the whole range. Instead, a flow regime-dependent model is required, as discussed in a later section.

When the liquid flow rates in two branches are different, Fig. 9(a) shows that the gas flow rate is less in the left channel where more water is injected and more gas flows in the right channel with less

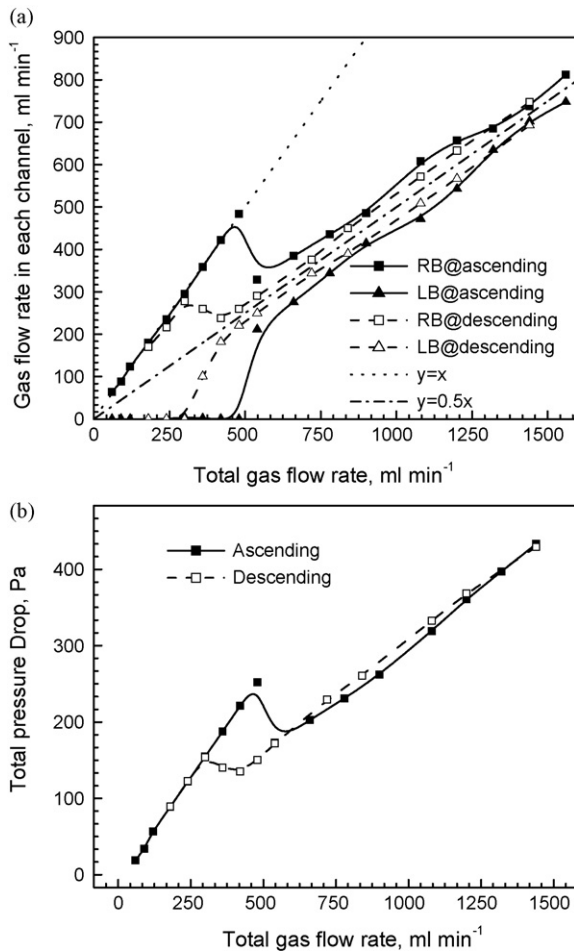


**Fig. 6.** (a) Gas flow rate in each channel and (b) total pressure drop as a function of total gas flow rate with  $u_L = 0.00055 \text{ m s}^{-1}$  in the left channel; solid line represents ascending approach and dotted line represents descending approach.

water present. The total pressure drop of two-phase at flow maldistribution conditions is generally higher than that at even flow distribution conditions, as shown in Fig. 9(b), which seems to be in disagreement with a speculation in the literature that a flow system always seeks a minimal pressure drop or energy state. According to our previous studies, we speculated that the flow distribution in a parallel channel system also depends on stability and previous history. The one observed in practice should be a stable state; otherwise, a disturbance will shift the unstable solution to a stable one.

### 3.3. Flow distribution dynamics

During each experiment, the pressure drop signals were recorded over about 1 min for the investigation of dynamics of gas flow distribution, with the typical signals for slug flow and annular flow being shown in Figs. 10 and 11, respectively. Fig. 10 shows that larger fluctuations in gas flow distribution are encountered at slug flow. The presence of periodic motion of liquid slugs blocks the passage of the gas flow and creates higher pressure drop, resulting in the flow of majority gas phase through the other channel with less flow resistance. In contrast, at the annular flow regime, the gas phase passes through a core surrounded by a thin liquid film; fluctuations are mainly attributed to the formation of a wavy interface between the core and annular region and as shown in Fig. 11. The implication for fuel cell operations is that slug flow should be avoided in order to achieve uniform gas distribution in parallel gas flow channels.

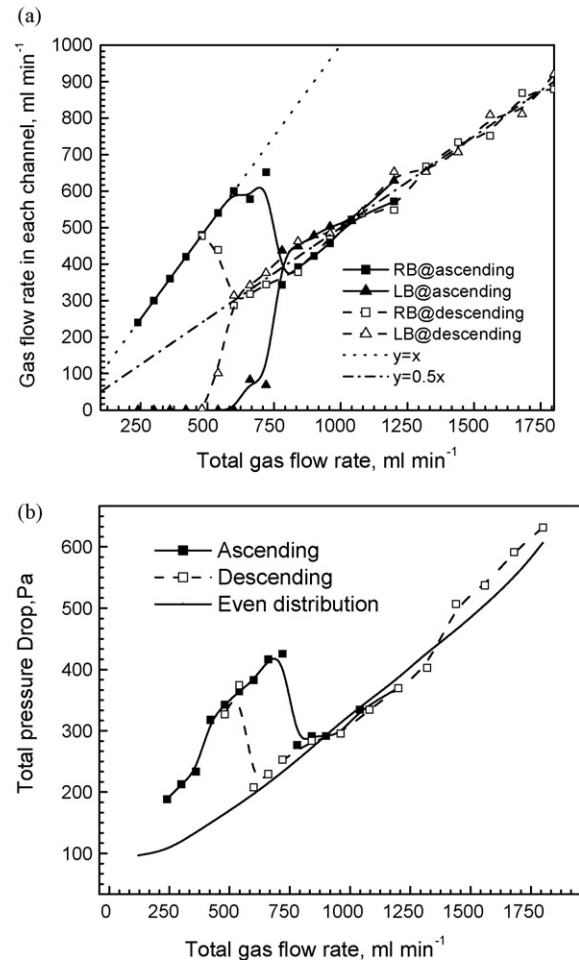


**Fig. 7.** (a) Gas flow in each channel and (b) corresponding total pressure drop as a function of total gas flow rate following both gas ascending and descending processes with equal liquid injection rates into two branches ( $u_{LR} = 0.00165 \text{ m s}^{-1}$  and  $u_{LL} = 0.00165 \text{ m s}^{-1}$ ).

## 4. Theoretical analysis

### 4.1. Comparison with correlations and models

There has been no attempt reported in the literature to predict two-phase flow distributions in parallel channels. In this section, an attempt was made to establish a mechanistic model to predict flow distribution in parallel channels. In line with our experimental work, the emphasis will be placed on a parallel channel system which shares the same inlet and outlet, implying that flow distributions must satisfy the equal pressure drop in both channels. In addition, conservation of mass is to be satisfied. In order to evaluate the two-phase pressure drop, a suitable model is required. There have been many correlations or models available in the literature to predict pressure drops of two-phase flow in mini- and micro-channels. Among those correlations or models, Lockhardt–Martinelli (LM) model and homogeneous model are used most commonly. A comprehensive review of previous correlations or models is beyond the scope of this work. Instead, models used in the current work for comparison with our experimental data are briefly presented as follows:

#### 4.1.1. Lockhardt–Martinelli model [9]

Based on the separated flow model, Lockhardt–Martinelli proposed the following correlation to calculation two-phase frictional

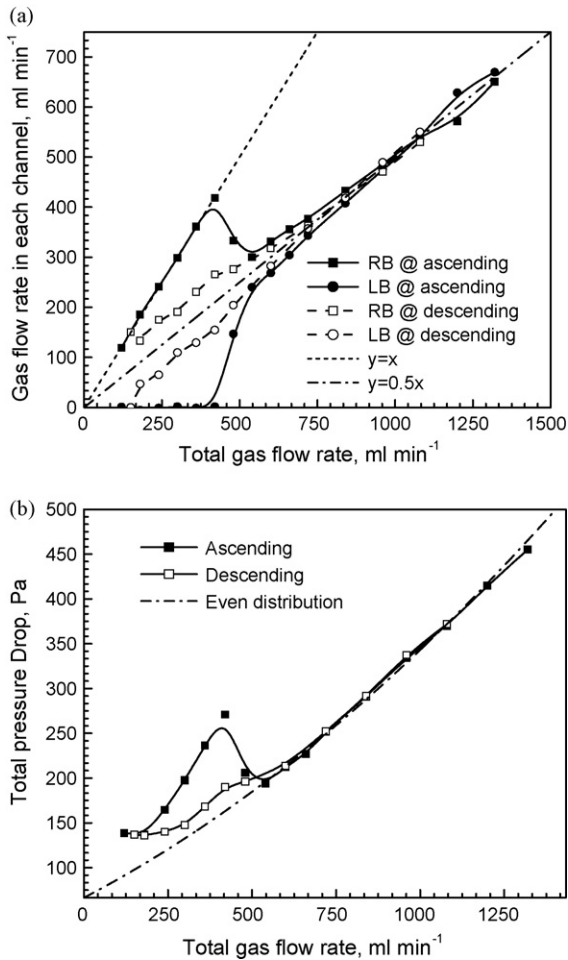


Fig. 8. (a) Flow distributions and (b) corresponding pressure drop with the same liquid flow rates in two channels ( $u_{LR} = 0.00055 \text{ m s}^{-1}$  and  $u_{LL} = 0.00055 \text{ m s}^{-1}$ ).

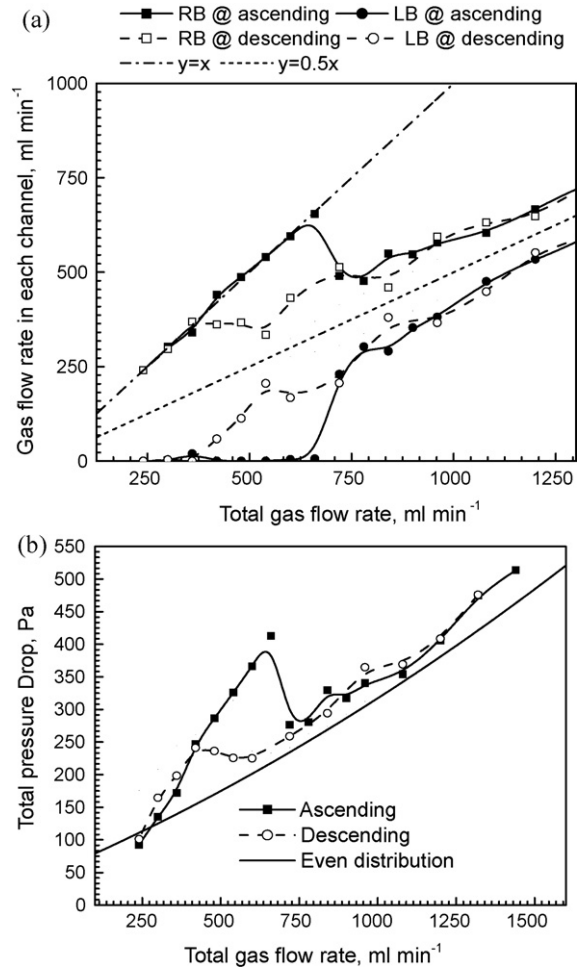


Fig. 9. (a) Gas flow distributions and (b) corresponding pressure drop with different liquid flow rates in two branches ( $u_{LR} = 0.0011 \text{ m s}^{-1}$  and  $u_{LL} = 0.0022 \text{ m s}^{-1}$ ).

pressure drop related to the pressure drop in a single-phase flow:

$$\phi_G^2 = \frac{\Delta P_{GL}}{\Delta P_G} \quad (3)$$

$$\phi_L^2 = \frac{\Delta P_{GL}}{\Delta P_L} \quad (4)$$

$$\phi_{LO}^2 = \frac{\Delta P_{GL}}{\Delta P_{LO}} \quad (5)$$

where  $\phi^2$  is the two-phase multiplier, the subscripts L and G refer to the pure liquid and pure gas phases flowing through the whole channel, respectively, LO refers to the entire fluid flow as a liquid phase through the channel with the same amount of mass flux. Those multipliers are often correlated in terms of the Martinelli parameter:

$$\chi^2 = \frac{\Delta P_L}{\Delta P_G} \quad (6)$$

$\Delta P_{GL}$  is the pressure drop in a two-phase flow system, Pa, while  $\Delta P_G$  is the pressure drop for a single-phase gas flow system, Pa. Chisholm correlated the multipliers with the parameter  $\chi^2$  as follows [10]:

$$\phi_G^2 = 1 + C\chi + \chi^2 \quad (7)$$

where C is flow regime-dependent parameter, for typical laminar gas and laminar liquid flows,  $C=5$ . However, English and Kandlikar found that in minichannels with diameters around 1 mm, LM approach with  $C=5$  generally overestimated their pressure drop

data for laminar gas and laminar liquid flows [11]. Based on a correlation developed by Mishima and Hibiki [12], they proposed a modified Chisholm constant C for non-circular minichannels:

$$C = 5[1 - \exp(-319D_h)] \quad (8)$$

where  $D_h$  is the hydraulic diameter of the channel in mm.

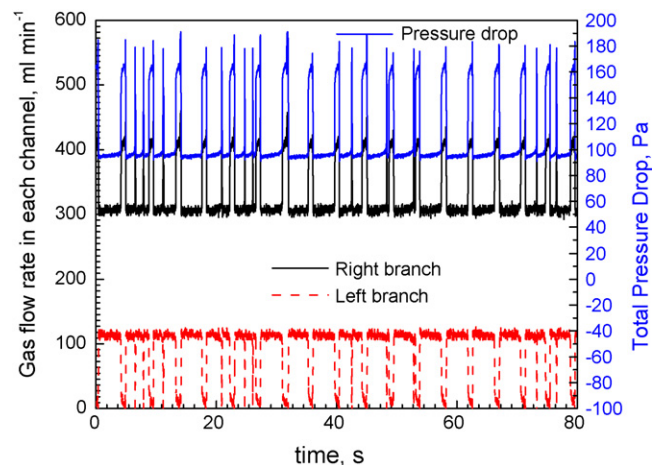


Fig. 10. Dynamic gas flow distributions at  $Q_G = 420 \text{ ml min}^{-1}$  and  $u_L = 0.00055 \text{ m s}^{-1}$  (slug flow).

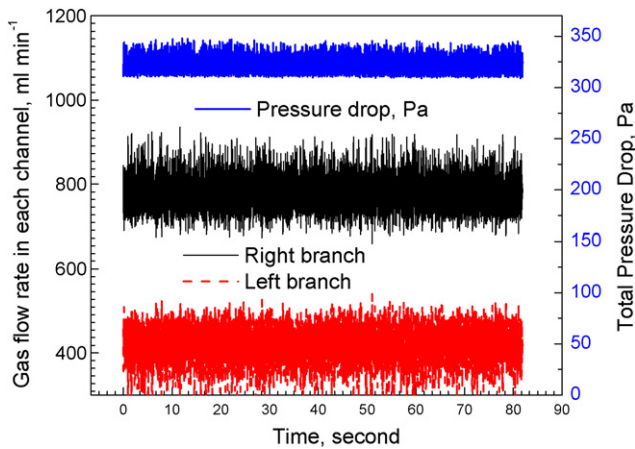


Fig. 11. Dynamic gas flow distributions at  $Q_G = 1200 \text{ ml min}^{-1}$  and  $u_L = 0.0033 \text{ m s}^{-1}$  (annular flow).

Tran et al. [13] proposed the following correlation to predict two-phase flow pressure drop:

$$\phi_{LO}^2 = 1 + (4.3x^2 - 1)(La(1-x)^{0.875} + x^{1.75}) \quad (9)$$

where  $x$  is the mass quantity, i.e., mass fraction of gas phase.

$La$  is the Laplace number and is evaluated by the following equation:

$$La = \frac{(\sigma/g(\rho_L - \rho_G))^{0.5}}{D_h} \quad (10)$$

Sun and Mishima developed a correlation to account for slip effect of two phases as follows [14]:

$$C = 1.79 \left( \frac{Re_G}{Re_L} \right)^{0.4} \left( \frac{1-x}{x} \right)^{0.5} \quad (11)$$

Muller-Steinhagen and Heck proposed the following equation [15]:

$$\frac{\Delta P_{GL}}{L} = F(1-x)^{1/3} + \left( \frac{\Delta P}{L} \right)_{LO} x^3 \quad (12)$$

where

$$F = \left( \frac{\Delta P_L}{L} \right)_{LO} + 2 \left[ \left( \frac{\Delta P}{L} \right)_{GO} - \left( \frac{\Delta P}{L} \right)_{LO} \right] x \quad (13)$$

#### 4.1.2. Homogenous model

The homogeneous model is another commonly used method for two-phase flows by treating the two-phase flow as a single-phase flow system with mixed physical properties such as density and viscosity. Therefore, the same equation for the pressure drop in a

Table 1  
Comparison of predictions from evaluated correlations.

Correlations or models	MARR
LM with $C=5$	55.6%
English and Kandlikar [11]	14.4%
Tran et al. [13]	48.5%
Muller-Steinhagen and Heck [15]	13.3%
Mishima and Hibiki [12]	109%
Sun and Mishima [14]	166%
Eq. (14)	10.5%
Homogeneous model	19.8%
Garimella et al. [16]	61.7%

single-phase flow is employed:

$$\frac{\Delta P_{GL}}{L} = \frac{2f_{TP}G^2}{\rho_{TP}D_h} \quad (14)$$

$G$  is the mass flux in  $\text{kg m}^{-2} \text{ s}^{-1}$ .

If  $Re_{TP}$  is less than 2100, for a square channel, similar to a single-phase flow, the frictional factor,  $f_{TP}$ , can be evaluated for a square cross-section by

$$f_{TP} = \frac{57}{Re_{TP}} \quad (15)$$

with the mixture density,

$$\rho_{TP} = \left( \frac{x}{\rho_G} + \frac{1-x}{\rho_L} \right)^{-1} \quad (16)$$

Comparisons between previous models and the current experimental pressure drop data were conducted with the results shown in Fig. 12. A mean averaged relative residue (MARR) is employed to indicate the deviation between predictions from existing correlations and experimental data as shown in Table 1.

It is seen that correlations of Mishima and Hibiki [12], Tran et al. [13], Sun and Mishima [14], and LM with  $C=5$  generally over-predict our experimental data. The model from Garimella et al. [16] underestimates our experimental data at low pressure drops where slug flow pattern prevails due to that the model was developed for annular flows. In contrast, the models of English and Kandlikar [11], homogenous model, Muller-Steinhagen and Heck [15] show good agreement with our experimental data and deviations are generally within 20% as shown in Table 1. A modified model from Sun and Mishima [14] is also proposed as shown in Eq. (17) with the lowest deviation of only 10.5%:

$$C = 0.23 \left( \frac{Re_G}{Re_L} \right)^{0.4} \left( \frac{1-x}{x} \right)^{0.5} \quad (17)$$

Large deviations between existing models or correlations and our experimental pressure drop data indicate that caution should be exercised, especially at mass flux lower than  $20 \text{ kg m}^{-2} \text{ s}^{-1}$ ,



Fig. 12. Comparison between predicted and measured two-phase pressure drop data by various correlations or models: (a) models with small deviations and (b) models with large deviations.

which represents typical two-phase operating conditions in PEM fuel cells. At low mass fluxes, smaller  $C$  values reflect weak interactions between gas and liquid phases in terms of pressure drop contributions. In addition, it should be noted that all models do not work for the whole range of flow conditions. Slightly wider scattering of predictions is found at lower pressure drops in the present study, indicating that flow pattern-dependent pressure drop models are likely to give improved predictions.

4.2. A new approach for the prediction of two-phase pressure drop in parallel channels

To predict gas flow rate distribution in parallel channels, a new approach is developed based on flow pattern-dependent pressure drop models. Two major flow regimes are considered in this work: bubbly/slug flows and annular/stratified flows.

The identical pressure drop of parallel channels sharing the same inlet and outlet requires

$$\Delta P_1 = \Delta P_2 \tag{18}$$

where  $\Delta P_1$  and  $\Delta P_2$  are the total pressure drop in two channels, Pa, respectively.

For channel 1:

$$\Delta P_1 = \Delta P_{G1} + \Delta P_{GL1} \tag{19}$$

where  $\Delta P_{G1}$  is the pressure drop of the entrance section without the presence of water, Pa, and  $\Delta P_{GL1}$  is the pressure drop of two-phase flow section after the entrance region, Pa.

Similarly, for channel 2:

$$\Delta P_2 = \Delta P_{G2} + \Delta P_{GL2} \tag{20}$$

For single-phase gas flow in a single minichannel with a square cross-section, the pressure drop can be evaluated by the following equation under laminar flow conditions:

$$\Delta P_{Gi} = \frac{28.4u_{Gi}\mu_{GL0}}{D_h^2} \tag{21}$$

where  $i$  refers to channel  $i$ .

In addition, conservation of mass for the gas phase reads:

$$Q_0 = Q_1 + Q_2 \tag{22}$$

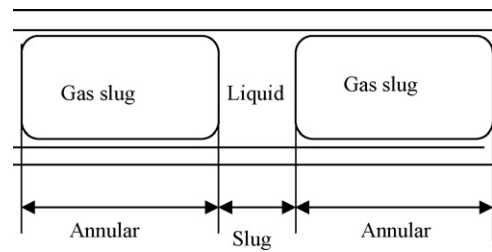


Fig. 13. Unit cell concept for pressure drop calculation in slug flows.

where  $Q_0$  is the total gas flow rate,  $\text{ml min}^{-1}$ , and  $Q_1$  and  $Q_2$  are gas flow rate in channels 1 and 2,  $\text{ml min}^{-1}$ , respectively.

For slug flows, a unit cell model is adopted to predict the pressure drop as depicted in Fig. 13 in which the pressure drop is divided into two portions. One is contributed by the liquid slug and the other is from the gas slug between two consecutive liquid slugs. The proportion of each contribution depends on length of liquid and gas slugs, which can be approximated by the phase holdup of each phase.

The following equation is used to evaluate the pressure drop of two-phase flow in slug flows:

$$\Delta P_{GL} = 4f_L \frac{L}{D_h} \frac{\rho_L(u_L + u_{Gi})^2}{2} (1 - \varepsilon_G) + 4f_{GL} \frac{L}{D_h} \frac{\rho_G(u_{Gi})^2}{2} \varepsilon_G \tag{23}$$

where  $f_L$  and  $f_{GL}$  are the frictional factors for liquid slugs and gas slug flows. The single liquid phase frictional factor,  $f_L$ , can be calculated in Eq. (15) with the Reynolds number based on the slug velocity ( $=u_L + u_{G1}$ ). The void fraction in the above equation is estimated by [4]:

$$\varepsilon_G = \frac{0.22\beta_G^{0.5}}{1 - 0.78\beta_G^{0.5}} \tag{24}$$

where  $\varepsilon_G$  and  $\beta_G$  are void fraction and no-slip void fraction, respectively.

The gas slug flow is treated as the same as the annular flow in view of that a liquid film presents in both cases, with the two-phase pressure drop calculated by

$$\Delta P_{GL} = 4f_{GL} \frac{L}{D_h} \frac{\rho_G(u_{G1})^2}{2} \tag{25}$$

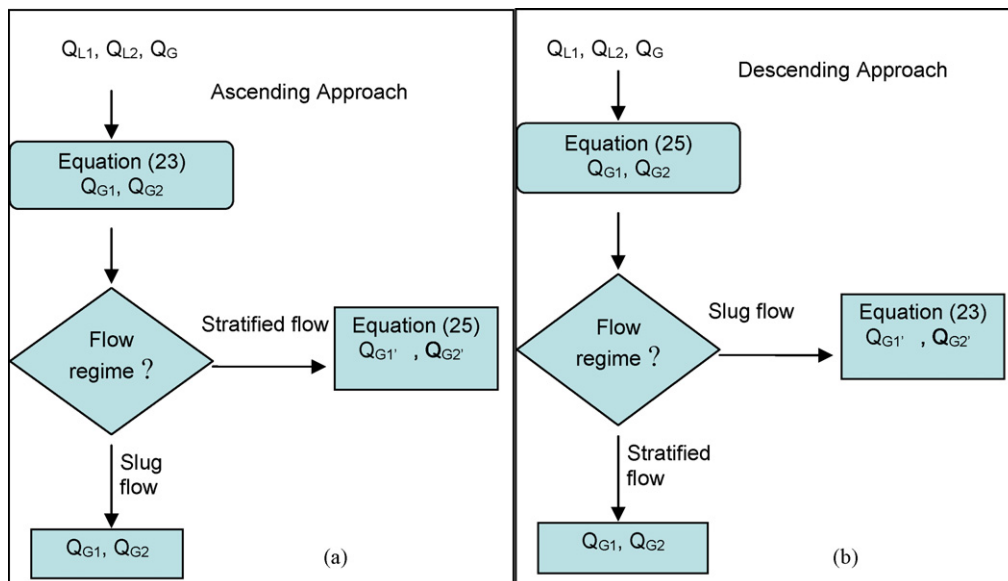
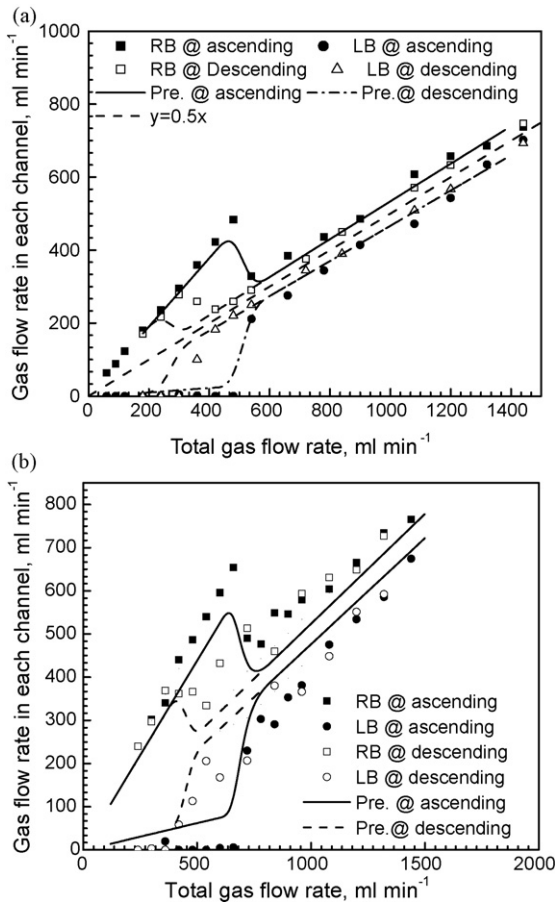


Fig. 14. Model calculation procedure for (a) ascending approach and (b) descending approach.



**Fig. 15.** Comparisons of predicted gas flow distributions with experimental data: (a)  $u_{LR} = 0$  and  $u_{LL} = 0.00055 \text{ m s}^{-1}$  and (b)  $u_{LR} = 0.0011 \text{ m s}^{-1}$  and  $u_{LL} = 0.0022 \text{ m s}^{-1}$ .

where the two-phase flow frictional factor,  $f_{GL}$ , is estimated by the Lockhart–Marinelli method with  $C$  estimated from Eq. (17):

$$\frac{f_{GL}}{f_G} = 1 + \frac{C}{\chi} + \chi^2 \quad (26)$$

The calculation procedure is schematically described in Fig. 14.

As shown in Fig. 14(a), in the ascending approach, at a given total gas flow rate, Eq. (23) is used to calculate the two-phase pressure drop in the channel with water injection while Eq. (25) is employed to calculate pressure drop in the other channel without water injection. The gas flow rate distributions,  $Q_{G1}$  and  $Q_{G2}$ , are then obtained from Eqs. (18)–(22). Flow regimes will be checked based on the resulted flow distributions and flow regime diagrams developed in a single channel system. If the slug flow does not hold and the two-phase flow falls into a stratified flow, Eq. (25) will be used to predict two-phase pressure drop in the channel receiving water injection to yield a new set of flow distribution,  $Q_{G1'}$  and  $Q_{G2'}$ . The above process is repeated when increasing gas flow rates. In contrast, in the descending approach, as indicated in Fig. 14(b), Eq. (25) is used to calculate the two-phase flow pressure drop in the channel with water injection. Subsequently, the flow pattern will be checked and if the stratified flow does not hold based on the resulted gas flow rates,  $Q_{G1}$  and  $Q_{G2}$ , Eq. (23) will be used to obtain a new set of flow rates,  $Q_{G1'}$  and  $Q_{G2'}$ .

According to the aforementioned procedure, flow distributions and corresponding pressure drops were predicted and compared with experimental data in Figs. 15 and 16.

It can be seen in Figs. 15 and 16 that the method developed in the current work can properly predict gas flow distributions in parallel channels once the liquid flow rates into each channel are speci-

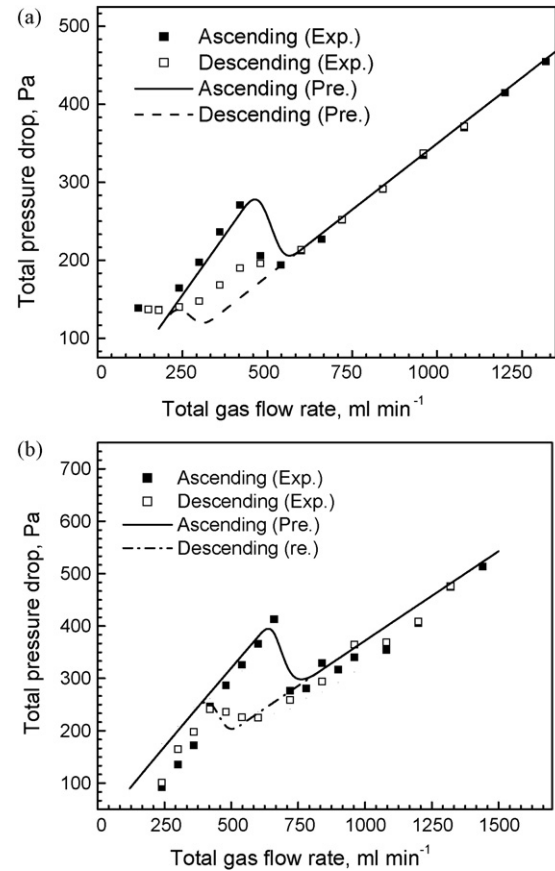


**Fig. 16.** Comparisons of predicted two-phase pressure drops and experimental data. (a)  $u_{LR} = 0$  and  $u_{LL} = 0.00055 \text{ m s}^{-1}$  and (b)  $u_{LR} = 0.0011 \text{ m s}^{-1}$  and  $u_{LL} = 0.0022 \text{ m s}^{-1}$ .

fied. The phenomena of flow hysteresis and multiplicity of flow distributions of two-phase flows can be captured by adopting flow regime-dependent pressure drop models in different experiments. The present study also implies that flow distributions of multiphase flow is not only determined by flow conditions, gas and liquid flow rates, but also considerably related to flow history and stability. We speculate that the non-linear relationship between pressure drop and gas flow rates plays a determinant role in gas and liquid flow distributions of such a parallel flow system. From our previous work, it was found that pressure drop does not monotonically increase with increasing gas flow rate [4]. A negative slope of pressure drop against gas flow rate was observed, corresponding to the region with flow pattern transitions. The concept of minimal pressure drop does not hold since the observed pressure drop for non-uniform distribution is generally higher than that of an even distribution. The current approach for the first time presents a possible explanation of the phenomenon and serves as a potential tool for predicting two-phase flow distribution in parallel channels, particularly, for fuel cells once the liquid flow rate into each channel is pre-determined, e.g. based on the water formation rates in active fuel cells. The method is also applicable to multiple parallel channels other than two with/without the same geometries. Similarly, for a system with more than two channels, flow regimes in individual channels need to be checked based on their gas and liquid flow rates. Therefore, increased computational cost will be needed with an increase in the number of channels. In addition, one limitation of the current approach is that the liquid flow rates in each channel need to be specified or pre-determined due to the unique liquid injection method. A fully predictive approach is still needed when neither the gas nor the liquid flow rate in each channel is specified or pre-determined. Moreover, to improve the accuracy



of the method, better two-phase pressure drop models need to be developed, especially for flows of low gas and liquid flow rates. A two-phase pressure drop model in minichannels accounting for channel wettability and porous wall also needs to be developed in order to apply this method to active fuel cells in the future.

## 5. Conclusions

In the present study, gas flow rates in individual minichannels were obtained in gas–liquid two-phase flows through measured pressure drops over the entrance region. Flow hysteresis was evidenced by gas flow distributions and pressure drops of two-phase flow in two different experiments conducted in ascending and descending orders. Effects of liquid flow rates on gas flow rates were investigated. It was found that gas flow distribution considerably relies on liquid flow rates and liquid flow distributions. Comparison of existing correlations for pressure drop predictions shows that weak interaction between gas and liquid phases at low mass flux results in large deviations from previous correlations. A new method was developed to explain the mal-distribution of gas–liquid two-phase flow in parallel channels and was applied to predict flow distributions of two-phase flow in parallel channels based on flow pattern-dependent pressure drop models. Multiplicity and flow hysteresis of two-phase flow in parallel channels can be successfully captured by the developed method.

## Acknowledgements

The authors are grateful for a strategic grant from the Natural Sciences and Engineering Research Council of Canada (NSERC) to support this work.

## References

- [1] K. Tüber, D. Póca, C. Hebling, J. Power Sources 124 (2003) 403–414.
- [2] I.S. Hussani, C.Y. Wang, J. Power Sources 187 (2009) 444–451.
- [3] Y. Wang, S. Basu, C.Y. Wang, J. Power Sources 179 (2008) 603–617.
- [4] L.F. Zhang, H.T. Bi, D.P. Wilkinson, J. Stumper, H.J. Wang, J. Power Sources 183 (2008) 643–650.
- [5] Z. Lu, S.G. Kandlikar, C. Rath, M. Grimm, W.E. Domigan, A.D. White, M. Hardberger, J.P. Owejan, T.A. Trabold, Int. J. Hydrogen Energy 34 (2009) 3445–3456.
- [6] S.G. Kandlikar, Z. Lu, W.E. Domigan, A.D. White, M.W. Benedict, Int. J. Heat Mass Transfer 52 (2009) 1741–1752.
- [7] M. Ozawa, K. Akagawa, K. Skaguchi, Int. J. Multiphase Flow 15 (1989) 639–657.
- [8] L.F. Zhang, W. Du, H.T. Bi, D.P. Wilkinson, J. Stumper, H.J. Wang, J. Power Sources 189 (2009) 1023–1031.
- [9] R.W. Lockhardt, R.C. Martinelli, Chem. Eng. Prog. 45 (1949) 39–48.
- [10] D. Chisholm, Int. J. Heat Mass Transfer 10 (1967) 767–1778.
- [11] N.J. English, S.G. Kandlikar, Heat Transfer Eng. 27 (2006) 99–109.
- [12] K. Mishima, T. Hibiki, Int. J. Multiphase Flow 22 (1996) 703–712.
- [13] T.N. Tran, M.C. Chyu, M.W. Wambasganss, D.M. France, Int. J. Multiphase flow 26 (2000) 1739–1754.
- [14] L.C. Sun, K. Mishima, Int. J. Multiphase Flow 35 (2009) 47–54.
- [15] H. Muller-Steinhagen, K. Heck, Chem. Eng. Prog. 20 (1986) 297–308.
- [16] S. Garimella, A. Agarwal, J.D. Killion, Heat Transfer Eng. 26 (2005) 28–35.